



Published in final edited form as:

Circ Res. 2017 June 23; 121(1): 56–70. doi:10.1161/CIRCRESAHA.117.310870.

Myeloperoxidase Mediates Postischemic Arrhythmogenic Ventricular Remodeling

Martin Mollenhauer^{1,2}, Kai Friedrichs^{1,2}, Max Lange^{1,2}, Jan Gesenberg^{1,2}, Lisa Remane^{1,2}, Christina Kerkenpaß^{1,2}, Jenny Krause³, Johanna Schneider^{1,2}, Thorben Ravekes^{1,2}, Martina Maass^{1,2}, Marcel Halbach^{1,2}, Gabriel Peinkofer^{1,2}, Tomo Saric^{1,4}, Dennis Mehrkens^{1,2}, Matti Adam^{1,2}, Florian G. Deuschl⁵, Denise Lau³, Birgit Geertz⁶, Kashish Manchanda^{1,2}, Thomas Eschenhagen⁶, Lukas Kubala^{7,8}, Tanya K. Rudolph^{1,2}, Yuping Wu⁹, W.H. Wilson Tang¹⁰, Stanley L. Hazen¹⁰, Stephan Baldus^{1,2}, Anna Klinke^{1,2,8}, and Volker Rudolph^{1,2}

¹Cardiology, Heart Center, University of Cologne, Cologne, Germany

²Center for Molecular Medicine Cologne, University of Cologne, Cologne, Germany

³University Heart Center Hamburg, Hamburg

⁴Center for Physiology and Pathophysiology, Institute for Neurophysiology, Medical Faculty, University of Cologne, Germany

⁵General and Interventional Cardiology, University Heart Center Hamburg, University Hospital Hamburg-Eppendorf (UKE), Hamburg, Germany

⁶Experimental Pharmacology and Toxicology, University Heart Center Hamburg, University Hospital Hamburg-Eppendorf (UKE), Hamburg, Germany

⁷Institute of Biophysics, Czech Academy of Sciences, Brno, Czech Republic

⁸International Clinical Research Center, St. Anne's University Hospital Brno, Brno, Czech Republic

⁹Mathematics, Cleveland State University, Cleveland, USA

¹⁰Cellular and Molecular Medicine and Cardiovascular Medicine, Cleveland Clinic, Cleveland, USA

Abstract

Rationale—Ventricular arrhythmias remain the leading cause of death in patients suffering myocardial ischemia. Myeloperoxidase (MPO), a heme-enzyme released by polymorphonuclear

Address correspondence to: Dr. Volker Rudolph, Heart Center, University of Cologne, Kerpener Strasse 62, 50937 Cologne, Tel.: +49-221-47832412, Fax: +49-221-47832400, volker.rudolph@uk-koeln.de.

M.M., K.F., M.L., J.G., A.K., and V.R. contributed equally to this study.

Disclosure: Dr. Hazen reports being named as co-inventor on pending and issued patents held by the Cleveland Clinic relating to cardiovascular diagnostics and therapeutics. Dr. Hazen reports having been paid as a consultant for the following companies: Esperion, P&G. Dr. Hazen reports receiving research funds from Abbott, P&G, Pfizer Inc., Roche Diagnostics and Takeda. Dr. Hazen reports having the right to receive royalty payments for inventions or discoveries related to cardiovascular diagnostics or therapeutics from Cleveland Heart Lab., Siemens, Esperion, and Frantz Biomarkers, LLC.

neutrophils, accumulates within ischemic myocardium and has been linked to adverse left ventricular remodeling.

Objective—To reveal the role of MPO for the development of ventricular arrhythmias.

Methods and Results—In different murine models of myocardial ischemia MPO deficiency profoundly decreased vulnerability for ventricular tachycardia (VT) upon programmed right ventricular and burst stimulation and spontaneously as assessed by ECG telemetry following isoproterenol injection. Experiments employing CD11b/CD18-integrin-deficient (*CD11b^{-/-}*) mice and intravenous MPO infusion revealed that neutrophil infiltration is a prerequisite for myocardial MPO accumulation. Ventricles from MPO-deficient (*Mpo^{-/-}*) mice showed less pronounced slowing and decreased heterogeneity of electrical conduction in the periinfarct zone than WT mice. Expression of the redox sensitive gap-junctional protein connexin43 (Cx43) was reduced in the periinfarct area of WT compared to *Mpo^{-/-}* mice. In isolated WT cardiomyocytes, Cx43 protein content decreased upon MPO/H₂O₂-incubation. Mapping of induced pluripotent stem-cell-derived cardiomyocyte (iPSCM) networks and in vivo investigations linked Cx43 breakdown to MPO-dependent activation of matrix-metalloproteinase 7. Moreover, *Mpo^{-/-}* mice showed decreased ventricular postischemic fibrosis reflecting reduced accumulation of myofibroblasts. *Ex vivo*, MPO was demonstrated to induce fibroblast-to-myofibroblast transdifferentiation by activation of p38 mitogen-activated protein kinases (MAPK) resulting in upregulated collagen generation. In support of our experimental findings, baseline MPO plasma levels were independently associated with a history of ventricular arrhythmias, sudden cardiac death, or implantable cardioverter defibrillator implantation in a cohort of 2622 stable patients with an ejection fraction above 35% undergoing elective diagnostic cardiac evaluation.

Conclusions—MPO emerges as a crucial mediator of post-ischemic myocardial remodeling, and may evolve as a novel pharmacological target for secondary disease prevention following myocardial ischemia.

Keywords

Ventricular tachycardia; connexin43; myocardial ischemia; inflammation; fibrosis; infarct or infarction; myeloperoxidase

Introduction

Sudden cardiac death is the leading cause of death following myocardial infarction and three quarters of patients dying from an acute arrhythmic event are diagnosed for coronary artery disease¹. Myocardial ischemia is one of the most powerful triggers of leukocyte recruitment and activation. In particular, neutrophils are among the first cells found in the area at risk and their activation in the setting of acute myocardial ischemia can be measured systemically. Upon activation, neutrophils release myeloperoxidase (MPO), a heme enzyme abundantly expressed in these cells. MPO until recently was solely viewed as part of the innate immune defense². However, MPO has been shown to promote potent pro-inflammatory vascular properties, facilitating the consumption of endothelial nitric oxide directly or by generation of potent reactive oxygen species (ROS)³. MPO has been demonstrated to be involved in myocardial remodeling following myocardial injury: MPO not only increased myocardial collagen deposition following ligation of the left anterior

descending artery (LAD)⁴, MPO-deficient (*Mpo*^{-/-}) mice exhibited less left ventricular (LV) dilatation and attenuated impairment in systolic LV function⁵. In the atria, MPO also increased fibrotic remodeling, which was linked to an increased susceptibility to atrial fibrillation⁶. Apart from ventricular fibrosis there is indirect evidence that MPO promotes the degradation of the gap-junctional protein connexin 43 (Cx43), which has been firmly linked to ventricular arrhythmogenesis. Thus, Cx43 availability has been shown to be essentially determined by matrix-metalloproteinase 7 (MMP-7), an enzyme, whose activation has been shown to be regulated by MPO^{7,8}.

Herein, we show that systemic levels of MPO are associated with a history of ventricular arrhythmias in patients undergoing elective diagnostic cardiac evaluation, and that MPO is causally linked to arrhythmogenic ventricular remodeling in mice. A pro-arrhythmogenic role for MPO was observed in vivo using *Mpo*^{-/-} mice following either myocardial ischemia / reperfusion (I/R) injury or permanent ischemia (PI), revealing a role for MPO in both the enzymatic degradation of connexin43 (Cx43) and the propagation of ventricular fibrosis through induction of fibroblast-to-myofibroblast transdifferentiation, which are both hallmarks of pro-arrhythmogenic myocardial remodeling^{9,10}.

Methods

An expanded Methods section can be found in the Online Supplement.

Animal studies

Male, 8- to 12-week old wild type littermates (WT), MPO-deficient (*Mpo*^{-/-}) and CD11b/CD18-integrin-deficient (*CD11b*^{-/-}) mice were used for this study. Animals were littermates of C57BL/6J background. The strategy for the generation of *Mpo*^{-/-} mice has been previously reported^{11,12}. All animal studies were approved by the Universities of Hamburg and Cologne Animal Care and Use Committees and follow ARRIVE guidelines.

Left anterior descending artery ligation

In brief, 8- to 12-week old WT, *Mpo*^{-/-} and *CD11b*^{-/-} mice were subjected to left thoracotomy. An 8/0 polypropylene suture was placed through the myocardium into the anterolateral LV wall. For I/R the ligation was removed after 30 min to allow up to 7 days of reperfusion. For I/R of *CD11b*^{-/-} mice the ligation was removed after 40 min to allow up to 2 days of reperfusion. For PI mice were maintained for up to 21 days without reperfusion. Animals which died during instrumentations or which did not properly recover were excluded from analyses.

Right ventricular stimulation

After 7 days of reperfusion or 21 days of PI isoflurane anaesthetized WT, *Mpo*^{-/-} and *CD11b*^{-/-} mice were subjected to a protocol of right ventricular stimulation¹³. Ventricular tachycardia (VT) was defined as a series of repetitive ventricular ectopic beats lasting for more than 200 ms.

Implantation of ECG transmitters, ECG-telemetry, arrhythmia provocation

ECGs were recorded in freely moving unrestrained mice. 24 hrs after LAD ligation arrhythmia provocation was performed by double injections of isoproterenol (ISO, i.p. 2 mg/kg) separated by an interval of 30 minutes¹⁴. Ventricular tachycardia (VT) was defined as a series of repetitive ventricular ectopic beats lasting for more than 200 ms.

In-vivo electrophysiological mapping

After 7 days I/R or 21 days PI the heart was exposed by thoracotomy. A 32-electrode microelectrode array (Multichannel Systems, Reutlingen, Germany) was positioned on the epicardial surface of the left ventricle. Inhomogeneity index, absolute inhomogeneity, variation coefficient and mean velocity of interelectrode conduction were calculated¹⁵. For pacing studies the hearts were stimulated with a concentric bipolar electrode (FHC, Bowdoin, USA) with a stimulus rate of 10 Hz.

In-vitro electrophysiological mapping

Differentiation and purification of murine induced pluripotent stem cell-derived cardiomyocytes (iPSCM) is described elsewhere¹⁶. iPSCM at day 16 of differentiation were cultured on a 120-electrode microarray. After 5 days of settling cells were treated over night as indicated. Field potentials were recorded (120pMEA, Multichannel Systems) and activation maps were calculated as described above.

Echocardiographic studies

Transthoracic echocardiography was performed using the Vevo 2100 System (VisualSonics, Toronto, Canada).

AP recordings by sharp electrode

Short axis ventricular slices were prepared from hearts subjected to PI for 3 days as described before¹⁷. Intracellular action potential recordings (APs) were performed in ventricular slices with sharp electrodes (20-40 M Ω resistance when filled with 3 mol/l KCl) made of borosilicate glass capillaries (WPI, Sarasota, USA). For inhibitor experiments BaCl₂ (Sigma Aldrich, Germany) or Tetrodotoxin (Abcam, ab120054, Germany) was added, as indicated.

Determination of fibrotic area

Paraffin sections were stained with picosirius red following standard protocols. Images were acquired using a DP25 camera (Olympus, Hamburg, Germany) mounted on a BX51 microscope (Olympus). Mean fibrotic area of 12 sections was quantified using Cell A software (Olympus).

Determination of infarct size

Hearts were excised, cut into cross-sections and, for I/R analyses, incubated in 2,3,5-triphenyl-tetrazolium chloride solution (TTC), since additional Evans Blue perfusion is unfeasible with re-opened LAD. For PI, hearts were excised and injected with Evan's blue

dye via the aorta ascendens. Infarct area was assessed by planimetry using BZ2-Analyser software (Keyence).

Isolation and treatment of adult ventricular cardiomyocytes

Hearts were excised and mounted on a constant-flow Langendorff circulation (Radnoti Ltd., Ireland) and retrogradely perfused with Liberase TM (Roche) and trypsin (Invitrogen). Cells were collected and incubated with MPO (Planta Natural Products) and H₂O₂ (Sigma) and/or an inhibitor to MMP-7 (Calbiochem). Cells were lysed and processed for immunoblotting.

Murine MPO plasma levels

Heparin-plasma was analyzed for MPO using Mouse MPO-ELISA (Hycult Biotech).

Staining for polymorphonuclear neutrophil infiltration

Frozen heart sections (4 μm) were stained with rat anti-mouse neutrophil Ly6G primary antibody according to standard protocol. Images were acquired using a Prosilica GC camera (Allied Vision Technologies) mounted on a Leica DMLB light microscope.

Immunofluorescence staining for α-smooth muscle actin (α-SMA) and myeloperoxidase

Frozen heart sections (4 μm) were incubated with primary antibody against α-SMA (1:200, rabbit IgG) and DDR-2 (1:50, goat IgG) or myeloperoxidase (1:250, rabbit IgG) following secondary antibody incubation. Nuclei were stained with DAPI.

Fibroblast isolation, stimulation and analysis

Ventricles of WT mice were digested in Liberase/Tyrode's solution and cells were incubated for 8 hrs. For the analysis of phospho-p38 mitogen-activated protein kinase (MAPK) incubation time was reduced to 15 min. For the analysis of collagen type I incubation time was extended to 36 hrs. Unless otherwise indicated fibroblasts were treated with 10 μg/ml catalytically active or inactive MPO and 20 μM H₂O₂ or 10 μM p38-inhibitor SB203580. Fibroblasts were incubated with WT and *Mpo*^{-/-} leukocytes for 8 hrs. Cells were lysed and processed for immunoblotting

Immunoblotting for Cx43

Protein blotting was carried out with a modified standard protocol using primary antibodies to Cx43 (1:2000) or GAPDH (1:5,000). Cardiac HL-1 cells were treated with either PBS, MPO (10 μg/μl) + H₂O₂ (80 μM) and/or pro-MMP-7 (1 μg/ml) for 16 hrs.

Immunofluorescence staining for Cx43

Staining of frozen heart sections was carried out with a modified standard protocol detecting Cx43 and N-cadherin. Images were taken with a Retiga 1300 CCD camera mounted on Leica DMLB fluorescence microscope by iVision v4.0. The infarct region was identified by total absence of Cx43 immunoreactivity.

Cx43 and ion channel mRNA analyses

Left ventricular heart tissue was collected. RNA was isolated (RNeasy-Kit, Qiagen) and qRT-PCR (Sso Fast Eva Green, BioRad) was performed according to manufacturer's instructions. CT-values were normalized to CT-values of GAPDH.

MMP-7 activity

Left ventricular tissue was dissected to infarct and periinfarct tissue using a dissection microscope (Leica). Periinfarct tissue was analyzed for MMP-7 activity using the SensoLyte 520 MMP-7 Assay Kit (Anaspec) following manufacturer's instructions protocol.

Human MPO plasma levels

The study was approved by local ethics committees and was conducted in accordance to the Declaration of Helsinki and GCP requirements. All individuals gave written informed consent prior to inclusion in the study. Serum myeloperoxidase levels were assessed by CardioMPO (Cleveland Heart Lab, USA) assay on autoanalyzer according to manufacturer instructions.

Plasma cytokines

Plasma was analyzed for cytokines by using a LEGENDplex Mouse Inflammation Panel (13-plex, Biolegend) according to manufacturer's instructions.

Statistical analyses

Results are expressed as mean \pm standard deviation. Statistical analysis was performed, unless otherwise indicated, using Kruskal Wallis test followed by Bonferroni post hoc test, Mann-Whitney U test or unpaired Student's t-test as appropriate. Univariate and multivariate logistic regression analysis were used to determine independent predictors of arrhythmias, adjusting for traditional cardiac risk factors. Regression analyses were performed using JMP Pro version 10 (SAS Institute, Cary, North Carolina) and R (3.1.2, Vienna, Austria). All other calculations were carried out using SPSS version 23.0. $*=P<0.05$, $**=P<0.01$, $***=P<0.001$.

Results

MPO plasma levels, myocardial neutrophil infiltration and inflammatory response

To characterize a potential mechanistic link between MPO and the inducibility of ventricular arrhythmias (VT), different mouse models of myocardial ischemia were applied. Wild type (WT) and *Mpo*^{-/-} mice were subjected to ischemia and reperfusion (I/R) as well as permanent ischemia (PI) upon ligation of the *ramus interventricularis anterior* (LAD). MPO plasma levels were increased more than two-fold in WT mice both 7 d after I/R and 5 d after PI compared to sham-operated (sham) animals. After 21 days of PI MPO plasma levels dropped but were still significantly elevated in comparison to sham-operated animals (Figure 1A). Ly6G staining of the infarct and periinfarct zones revealed a significantly increased infiltration of PMN in WT animals compared to *Mpo*^{-/-} animals 7 days after I/R and, to a lesser, not significant extent, 3 days after PI (Figure 1B ,C). Of note, overall PMN

infiltration was lower after PI than after I/R. FACS analyses of multiple plasma cytokine levels at multiple time-points revealed no relevant differences between WT and *Mpo*^{-/-} mice in either model (Online Figure I).

Infarct size and left ventricular function

In accordance with previous reports, infarct size after 7 days I/R and 21 days after PI did not differ significantly between WT and *Mpo*^{-/-} mice. Expectedly, overall infarct size was much larger in hearts subjected to PI as compared to I/R (Figure 1D). In accordance, more pronounced deterioration of systolic left ventricular ejection fraction was observed after PI than after I/R at multiple time-points. No significant differences between WT and *Mpo*^{-/-} animals were noted at day 3 or 7 of I/R (Figure 1E), whereas upon PI, EF was improved in *Mpo*^{-/-} mice at day 21 (Figure 1F).

Importance of neutrophils for myocardial MPO accumulation

To investigate the role of altered myocardial neutrophil infiltration and MPO release on arrhythmia development after infarction, CD11b/CD18-integrin-deficient (*CD11b*^{-/-}) mice were subjected to I/R. Expectedly, *CD11b*^{-/-} mice showed a significantly reduced cardiac neutrophil infiltration as compared to WT littermates 6 hours and 2 days after I/R (Figure 1H, J). Importantly, despite elevated plasma levels of MPO in *CD11b*^{-/-} mice, which were similar to WT mice following I/R (Figure 1G), myocardial MPO levels were significantly lower than in WT mice (Figure 1I, K). Neither neutrophils nor intracardiac MPO could be detected after sham operation (*data not shown*). In line with these observations, supplementation of MPO via osmotic mini-pumps (*data not shown*) or daily retroorbital injections for 7 days did not result in myocardial accumulation of MPO within the left ventricle (Online Figure IIA right panel) despite supra-physiological plasma levels, suggesting that extravasation of neutrophils into the post ischemic tissues is of immanent importance to carry MPO into the myocardium.

Inducibility of VT by right ventricular stimulation

At day 7 of I/R and day 21 of PI WT mice exhibited increased vulnerability to VT (representative electrocardiograms (ECGs) in Figure 2A, B) as compared to sham-operated animals (WT sham) with respect to the number of VT episodes (Figure 2C) and the duration of VTs (Figure 2D). In comparison, *Mpo*^{-/-} mice undergoing I/R (*Mpo*^{-/-} I/R) or permanent LAD ligation (*Mpo*^{-/-} PI) showed a significantly reduced vulnerability for VT episodes and duration (Figure 2C, 2D). Over a period of 3 months following permanent LAD ligation no spontaneous deaths occurred and, accordingly, no difference in mortality between WT and *Mpo*^{-/-} mice after PI could be demonstrated (Online Figure III).

CD11b^{-/-} mice, which showed reduced neutrophil infiltration and cardiac MPO deposition after I/R subsection, were also significantly protected against VT induction as shown by a lower number and length of VT episodes as compared to WT mice (Figure 2E, F, G). Conversely, intravenous MPO infusion in *Mpo*^{-/-} mice, which was not associated with myocardial MPO accumulation, did not re-establish VT vulnerability in *Mpo*^{-/-} mice (Online Figure IIB, IIC).

Spontaneous VT development

To assess spontaneous VT development in vivo ECGs of WT and *Mpo*^{-/-} mice were recorded 24 hours after LAD-ligation and additional challenge with isoproterenol. *Mpo*^{-/-} mice showed a significantly less frequent development of spontaneous VT than WT (representative ECG traces are shown in Figure 2H). VT probability was lower, VT freedom was longer, VT number and mean time of VT episodes were lower (Figure 2I, J, K, L).

In vivo epicardial mapping studies

Epicardial mapping studies in spontaneously beating and stimulated hearts revealed a disruption of conduction homogeneity in WT animals following I/R and PI, whereas in *Mpo*^{-/-} mice it was preserved in both models, as ascertained by respective differences in the inhomogeneity index, absolute inhomogeneity, the variation coefficient of local phase delays and the mean conduction velocity (Figure 3). Of note no conduction was detectable within the infarct scar tissue in PI animals (data not shown).

Effects of MPO on expression and function of ion channels

Na_v1.5, Ca_v1.2, KV1.5, KVLQT1, Kir2.1, Kir6.2, TASK-1 and HCN2 transcripts were detectable within the infarct region 3 days after permanent LAD ligation. Furthermore, the levels of Na_v1.5, KV1.5, Kir6.2, TASK-1 and HCN2 mRNA was changed 3 days after LAD ligation as compared to myocardial tissue from healthy mice. Of importance, mRNA levels did not differ between WT and *Mpo*^{-/-} infarct tissue upon PI (Online Table I).

In addition, action potentials (AP) did not differ between WT and *Mpo*^{-/-} mice as assessed with sharp electrode measurements of living heart tissue slices after 7 days of PI apart from a shortened APD50 in *Mpo*^{-/-} mice (WT: 13.2±0.3 ms vs. *Mpo*^{-/-}: 9.5±1.4 ms; *P* 0.05). This is likely irrelevant given the absence of a significant effect on APD90 (WT: 88.8±6.0 ms vs. *Mpo*^{-/-}: 67.9±7.8 ms) or APD50/90 (WT: 15.3±0.9% vs. *Mpo*^{-/-}: 14.2±1.6%). To further characterize MPO's effects on ion channel function, increasing concentrations of ion channel blockers were administered to infarcted tissue slices of WT and *Mpo*^{-/-} animals. While the potassium channel blocker BaCl₂¹⁸ revealed no differences between both groups, AP amplitude was significantly decreased in hearts from *Mpo*^{-/-}-animals compared to WT animals after incubation with the sodium channel blocker tetrodotoxin¹⁹ (TTX; WT: 73.5±4.0 mV vs. *Mpo*^{-/-}: 47.6±5.5 mV; *P* 0.05, Online Figure IV).

Cx43 in the infarct- and periinfarct-zone

Since connexins, which allow for ion exchange between cardiomyocytes, are an integral part of myocardial conduction homogeneity and are regulated in a redox sensitive fashion, we tested the effect of MPO on Cx43 expression and function.

Immunostainings for Cx43 revealed a complete absence of Cx43 immunoreactivity in the infarct zone of WT and *Mpo*^{-/-} animals (Figure 4A). In the periinfarct region, a significantly decreased signal for Cx43 was detected in WT I/R mice compared to sham-operated mice. In contrast, no reduction was recognized in *Mpo*^{-/-} I/R mice in comparison to sham-operated *Mpo*^{-/-} mice (Figure 4B, 4C). Accordingly, *Mpo*^{-/-} hearts revealed significantly higher immunoreactivity for Cx43 in the periinfarct region 3 days and 21 days after PI induction

than WT hearts (Figure 4D, 4E). In both models, I/R and PI, ventricular Cx43 mRNA expression levels did not differ between WT and *Mpo*^{-/-} animals pointing towards a posttranslational effect of MPO on Cx43 levels (Figure 4F).

MMP-7 dependent Cx43 degradation

Studies in isolated adult cardiomyocytes confirmed a decreased content of Cx43 following incubation with MPO. Strikingly, this effect was partly reverted by additional treatment with an inhibitor of MMP-7, an enzyme not only shown to directly bind and degrade Cx43 following myocardial ischemia but also to be activated by MPO-derived hypochlorous acid (Figure 5A)^{7,8}. In addition, activation of MMP-7 was significantly more abundant in the periinfarct region of WT than in *Mpo*^{-/-} mice following I/R in vivo (Figure 5B). To further investigate the effect of MPO mediated Cx43 degradation via MMP-7 conduction patterns of a monolayer of induced pluripotent stem cell-derived cardiomyocytes (iPSCM) were assessed by in vitro mapping analyses. Importantly, these cells are devoid of MMP-7 as assessed by immunoblotting and quantitative real-time analysis (Online Figure V). Spontaneously beating iPSCM showed homogeneous conduction patterns (Figure 5C) under control conditions. Addition of MPO/H₂O₂ or pro-MMP-7 alone had no effect on the observed patterns. However, concomitant treatment with pro-MMP-7/MPO/H₂O₂ resulted in a severe disruption of conduction homogeneity as demonstrated by an increased inhomogeneity index (Figure 5D), an elevated absolute inhomogeneity (Figure 5E), an increased variation coefficient (Figure 5F) and a reduced mean conduction velocity (Figure 5G), indicative of diminished intercellular electrical coupling among iPSCM. Conversion of pro-MMP-7 to active MMP-7 by MPO-derived HOCl has been described before⁸. Accordingly, incubation of the cardiac muscle cell line HL-1, which also lacks MMP-7 protein expression (Online Figure V), with MPO/H₂O₂/pro-MMP-7 resulted in decreased Cx43 levels, whereas single treatment with MPO/H₂O₂ or pro-MMP-7 did not induce Cx43 degradation (Online Figure VI).

Ventricular fibrosis

Overall left ventricular fibrosis as well as interstitial ventricular fibrosis (excluding the infarct scar) 7 days after I/R were profoundly lower in *Mpo*^{-/-} mice than in WT animals, as demonstrated by myocardial picrosirius red stainings for collagen deposition (Figure 6A-C, Online Figure VII). Similarly, *Mpo*^{-/-} hearts exhibited significantly less fibrosis after 21 days of PI, albeit overall left ventricular fibrosis was again more pronounced than in the I/R model (Figure 6D, E, Online Figure VII).

Fibroblast-to-myofibroblast transdifferentiation

To determine myofibroblast accumulation in ventricular tissue, the main collagen-producing cell type in ventricular myocardium under pathological conditions²⁰, colocalization of the immunoreactivity for the fibroblast marker DDR2 and the myofibroblast marker α -SMA was assessed in cardiac sections 7 days after I/R and 5 days after PI. Indeed, the number of myofibroblasts was significantly lower in the infarct and periinfarct region of *Mpo*^{-/-} hearts than in WT after I/R or after PI. The total number of myofibroblasts was slightly but not significantly lower in WT I/R hearts than in WT PI hearts ($P=0.151$; Figure 7A, B). Immunoblot analyses revealed dose-dependent transdifferentiation of isolated cardiac

fibroblasts to myofibroblasts upon incubation with MPO in vitro. Strikingly, this equaled the effect of PDGF treatment, an established inducer of fibroblast differentiation (Figure 7C). The incubation of fibroblasts with MPO lead to a significantly increased expression of collagen type I compared to untreated cells (Figure 7D). Furthermore, co-culture of isolated fibroblasts with isolated WT leukocytes lead to a significantly more pronounced transdifferentiation of fibroblasts as compared to fibroblasts co-cultured with leukocytes isolated from *Mpo*^{-/-} mice (Figure 7E). Next, we tested whether MPO induces p38 mitogen-activated protein kinase (MAPK) phosphorylation in isolated fibroblasts, an inducer of fibroblast-to-myofibroblast transdifferentiation. Indeed, western blot analyses revealed an augmented amount of p38 MAPK phosphorylation upon MPO treatment, a process which was completely abolished upon additional p38-inhibitor treatment or treatment with catalytically inactive MPO (Figure 7F).

Systemic MPO levels are associated with ventricular arrhythmias

To test whether MPO is linked to the occurrence of arrhythmias in humans, we retrospectively measured circulating levels of MPO in a high-risk cohort of stable patients undergoing elective diagnostic cardiac evaluations during coronary angiography and who were no candidates for primary prevention ICD (ejection fraction above 35%)^{1,21}. Table 1 shows the baseline characteristics of the 2622 subjects included in the study cohort. The mean age of the population was 63.1±11.1 years, 76% of patients had coronary artery disease. Patients with arrhythmias were older, had a lower ejection fraction and more often received ACE inhibitors.. Binary logistic regression analysis revealed that MPO plasma levels are associated with a history of ventricular arrhythmias, sudden cardiac death and/or implantable cardioverter defibrillator implantation (OR: 1.76 (1.19-2.6) highest vs. lowest tertile) and remain correlated after adjustment for pertinent risk factors (1.83 (1.23-2.73) highest vs. lowest tertile; Table 2).

Discussion

Herein it is shown that MPO promotes proarrhythmic remodeling and ventricular arrhythmias following myocardial ischemia. Studies in two different animals models of ischemia-related myocardial damage using *Mpo*^{-/-} mice, and in vitro using spontaneously beating iPSCMs, reveal that MPO augments arrhythmogenic left ventricular remodeling as manifested in: i) breakdown of Cx43 by activation of MMP-7, and ii) enhanced ventricular fibrosis by transdifferentiation of fibroblasts, which ultimately leads to iii) pronounced electrical conduction slowing and disruption of conduction homogeneity, iv) and increased susceptibility to ventricular tachycardia.

The mechanisms underlying myocardial damage in I/R and PI are diverse²², but neutrophils have long been regarded as a crucial component^{23,24}. The neutrophil-derived enzyme MPO has been investigated in the context of ischemic myocardial damage. Vasilyev et al. showed that MPO-depletion had no effect on infarct size following myocardial I/R⁴, whereas Askari et al. demonstrated preserved left ventricular enddiastolic diameter (LVEDD) and left ventricular function in *Mpo*^{-/-} mice⁵. Instigated by these studies we were able to show that MPO also exerts pro-arrhythmogenic effects in the context of post-ischemic myocardial

remodeling. We identified Cx43 degradation and increased left ventricular fibrosis as underlying mechanisms for this observation. Cx43 is the principal gap-junctional protein in the left ventricle, which is critically linked to ventricular homogeneity of electrical conduction and ventricular arrhythmias²⁵. As outlined above, an important mechanism of periinfarct disruption of gap-junctional integrity is MMP-7-dependent degradation of Cx43⁷. MMP-7 has previously also been shown to be specifically activated by MPO⁸. Indeed, we were able to demonstrate reduced periinfarct MMP-7-activity in *Mpo*^{-/-} mice and abrogation of MPO-dependent Cx43 degradation by inhibition of MMP-7 in isolated adult murine cardiomyocytes. The dependence of MPO's effects on MMP-7 is strongly underlined by in vitro mapping studies of iPSC-derived cardiomyocytes: These cells do not express MMP-7, and indeed conduction homogeneity was not affected by MPO and H₂O₂ alone but only after addition of MPO/H₂O₂ and pro-MMP-7.

Fibrosis is regarded as a critical substrate for ventricular arrhythmias and MPO's profibrotic effects, e.g. by oxidative inactivation of plasminogen activator inhibitor-1 (PAI-1), have previously been demonstrated⁵. We therefore assessed ventricular fibrosis in our animal models and found that *Mpo*^{-/-} mice were protected from ventricular fibrosis. Since activation of MMP-7 is not involved in profibrotic remodeling after infarction,²⁶ we assessed fibroblast-to-myofibroblast transdifferentiation. Myofibroblasts maintain their secretory activity of collagen up to 90 days and are a significant component of progressive adverse cardiac remodeling²⁰. As evidenced by immunostainings of myocardial sections and functional in vitro studies, we could demonstrate MPO-dependent fibroblast transdifferentiation and could link this effect to MPO derived HOCl dependent p38 MAPK activation²⁷ thus disclosing a novel, additional profibrotic property of MPO.

Ion channel alterations in the periinfarct region have been demonstrated to be of relevance for ischemia-related cardiac arrhythmias²⁸. We have previously shown that MPO does not affect action potential characteristics in isolated cardiomyocytes⁶. Because studies on isolated cardiomyocytes only crudely approximate the conditions of cells integrated in the myocardial cell network within the periinfarct region we performed sharp-electrode measurements on living tissue slices of infarcted murine hearts and found no relevant differences between hearts from WT and *Mpo*^{-/-} mice. However, *Mpo*^{-/-} hearts showed an increased susceptibility to voltage-gated sodium channel inhibition by TTX as manifested by a decreased AP amplitude. This points towards post-translational modifications of voltage-gated sodium channels by MPO, which could be responsible for differences in susceptibility to arrhythmias. While further investigation of this interesting observation is clearly warranted the absence of an effect of MPO-deficiency on APs in untreated tissue slices as well as the strong effects of MPO-deficiency on Cx43 and fibrosis together with the reduced epicardial conduction velocity suggest a more dominant role for these latter mechanisms in the context of the current study.

It is of great interest for MPO's mode of action that infiltration of neutrophils appears to be required for accumulation of MPO in the ventricular myocardium as suggested by our studies on *CD11b*^{-/-} mice and MPO supplemented *Mpo*^{-/-} mice. Indeed, this observation could provide an additional explanation for the limited usefulness of MPO as a biomarker

for myocardial infarction, because MPO plasma levels might only partially correlate with local abundance of MPO.

Certainly, the current study bears some limitations: It remains open whether the mechanisms revealed herein will finally affect mortality in human pathophysiology: As shown previously, this animal model is not yielding significant mortality – in fact, we and others did not observe any deaths of mice upon 3 months following permanent ischemia^{29,30}. Moreover, the complex pathogenesis of ventricular arrhythmias upon myocardial ischemia, which is based on electrical remodeling of ion channels and calcium kinetics can only be in part appreciated in a mouse model. However, mouse models have been widely employed and have allowed broad insight into the pathogenesis of VTs when focusing on connexin dependent electrical homogeneity and fibrosis^{13,31,32,33}. Given the fact that MPO is much less expressed in murine PMN as compared to human neutrophils, the observed effects potentially underestimate the role of MPO in this disease in humans. In addition, it clearly has to be assumed that next to the specific effects of MPO on Cx43 and fibroblast transdifferentiation, which were evident in the absence of neutrophils in our in vitro experiments, MPO promotes perpetuation of local inflammation by its chemoattractant and neutrophil activating properties^{34,35}. In addition, other pathways, like oxidative inactivation of PAI-1 are known to contribute to the observed effects of MPO on fibrotic remodeling, as has previously been demonstrated⁵. A number of limitations also apply to our clinical observational data. Some baseline parameters were not balanced between both groups, which can only partly be corrected by multivariate analysis. In addition, MPO levels were only examined in subjects subjected to coronary angiography at one point in time at a single tertiary referral center; therefore, we cannot exclude selection bias for patients undergoing diagnostic cardiac catheterization. Given these limitations, the data can only be regarded as a pilot study and should be confirmed in independent cohorts. In addition, whether the prognostic value of MPO would be further increased upon serial MPO assessments remains unknown. Furthermore, the implementation of MPO as a biomarker to predict VT appears problematic because of the fact that plasma MPO levels will only in part reflect myocardial MPO activity. Thus, the clinical usefulness of MPO as a biomarker for arrhythmic events cannot be derived from the present data and needs to be further studied. However, the current data set comprises the largest population tested for an inflammatory biomarker indicating ventricular arrhythmogeneity, which in our view confirms the mechanistic data reported herein.

In conclusion, the current data reveal that MPO affects electrical conduction in the ischemic left ventricle and thereby increases the vulnerability for ventricular arrhythmias.

Mechanistically, MPO impairs Cx43 integrity through activation of MMP-7 and induces fibrotic remodeling by stimulating fibroblast transdifferentiation to myofibroblasts through activation of p38 MAPK. These results not only indicate that the innate immune system and namely leukocytes exert proarrhythmogenic properties, but also point towards MPO as a potential pharmacological target in this disease.

Supplementary Material

Refer to Web version on PubMed Central for supplementary material.

Acknowledgments

We thank Adnana Paunel-Görgülü for providing the HL-1 cells, Dirk Isbrandt for supporting the telemetry experiments and Christina Schroth and Katja Urban for expert technical assistance.

Sources of Funding: This work was supported by the Deutsche Forschungsgemeinschaft [KL 2516/1-1 to A.K.; BA 1870/7-1, BA 1870/9-1 and BA 1870/10-1 to S.B.; AD 492/1-1 to MA; RU 1876/1-1 and RU 1876/3-1 to V.R.]; The Ministry of Education, Youth and Sports CR [the National Program of Sustainability II no. LQ1605 to L.K.]; and the CMMC funding [Baldus 2-GA and B-02]. The GeneBank studies were supported by NIH grants P01HL076491, R01HL126827 and the Cleveland Clinic Clinical Research Unit of the Case Western Reserve University CTSA (UL1TR 000439).

References

1. Zipes DP, Camm AJ, Borggrefe M, Buxton AE, Chaitman B, Fromer M, Gregoratos G, Klein G, Moss AJ, Myerburg RJ, Priori SG, Quinones MA, Roden DM, Silka MJ, Tracy C. ACC/AHA/ESC 2006 Guidelines for Management of Patients With Ventricular Arrhythmias and the Prevention of Sudden Cardiac Death. *Circulation*. 2006; 114
2. Lau D, Baldus S. Myeloperoxidase and its contributory role in inflammatory vascular disease. *Pharmacol Ther*. 2006; 111:16–26. [PubMed: 16476484]
3. Abu-Soud HM, Hazen SL. Nitric oxide is a physiological substrate for mammalian peroxidases. *J Biol Chem*. 2000; 275:37524–32. [PubMed: 11090610]
4. Vasilyev N, Williams T, Brennan M-L, Unzek S, Zhou X, Heinecke JW, Spitz DR, Topol EJ, Hazen SL, Penn MS. Myeloperoxidase-generated oxidants modulate left ventricular remodeling but not infarct size after myocardial infarction. *Circulation*. 2005; 112:2812–20. [PubMed: 16267254]
5. Askari AT, Brennan M-L, Zhou X, Drinko J, Morehead A, Thomas JD, Topol EJ, Hazen SL, Penn MS. Myeloperoxidase and plasminogen activator inhibitor 1 play a central role in ventricular remodeling after myocardial infarction. *J Exp Med*. 2003; 197:615–24. [PubMed: 12615902]
6. Rudolph V, Andrié RP, Rudolph TK, Friedrichs K, Klinke A, Hirsch-Hoffmann B, Schwoerer AP, Lau D, Fu X, Klingel K, Sydow K, Didié M, Seniuk A, von Leitner E-C, Szoecs K, Schrickel JW, Treede H, Wenzel U, Lewalter T, Nickenig G, Zimmermann W-H, Meinertz T, Böger RH, Reichenspurner H, Freeman BA, Eschenhagen T, Ehmke H, Hazen SL, Willems S, Baldus S. Myeloperoxidase acts as a profibrotic mediator of atrial fibrillation. *Nat Med*. 2010; 16:470–4. [PubMed: 20305660]
7. Lindsey ML, Escobar GP, Mukherjee R, Goshorn DK, Sheats NJ, Bruce JA, Mains IM, Hendrick JK, Hewett KW, Gourdie RG, Matrisian LM, Spinale FG. Matrix metalloproteinase-7 affects connexin-43 levels, electrical conduction, and survival after myocardial infarction. *Circulation*. 2006; 113:2919–28. [PubMed: 16769909]
8. Fu X, Kassim SY, Parks WC, Heinecke JW. Hypochlorous acid oxygenates the cysteine switch domain of pro-matrilysin (MMP-7). A mechanism for matrix metalloproteinase activation and atherosclerotic plaque rupture by myeloperoxidase. *J Biol Chem*. 2001; 276:41279–87. [PubMed: 11533038]
9. Rubart M, Zipes DP. Mechanisms of sudden cardiac death. *J Clin Invest*. 2005; 115:2305–15. [PubMed: 16138184]
10. de Jong S, van Veen TAB, van Rijen HVM, de Bakker JMT. Fibrosis and Cardiac Arrhythmias. *J Cardiovasc Pharmacol*. 2011; 57:630–638. [PubMed: 21150449]
11. Brennan ML, Anderson MM, Shih DM, Qu XD, Wang X, Mehta AC, Lim LL, Shi W, Hazen SL, Jacob JS, Crowley JR, Heinecke JW, Lusis AJ. Increased atherosclerosis in myeloperoxidase-deficient mice. *J Clin Invest*. 2001; 107:419–30. [PubMed: 11181641]
12. Coxon A, Rieu P, Barkalow FJ, Askari S, Sharpe AH, von Andrian UH, Arnaout MA, Mayadas TN. A novel role for the beta 2 integrin CD11b/CD18 in neutrophil apoptosis: a homeostatic mechanism in inflammation. *Immunity*. 1996; 5:653–66. [PubMed: 8986723]
13. Roell W, Lewalter T, Sasse P, Tallini YN, Choi B-R, Breitbach M, Doran R, Becher UM, Hwang S-M, Bostani T, von Maltzahn J, Hofmann A, Reining S, Eiberger B, Gabris B, Pfeifer A, Welz A, Willecke K, Salama G, Schrickel JW, Kotlikoff MI, Fleischmann BK. Engraftment of connexin 43-expressing cells prevents post-infarct arrhythmia. *Nature*. 2007; 450:819–24. [PubMed: 18064002]

14. Vettel C, Lindner M, Dewenter M, Lorenz K, Schanbacher C, Riedel M, Lämmle S, Meinecke S, Mason FE, Sossalla S, Geerts A, Hoffmann M, Wunder F, Brunner FJ, Wieland T, Mehel H, Karam S, Lechêne P, Leroy J, Vandecasteele G, Wagner M, Fischmeister R, El-Armouche A. Phosphodiesterase 2 Protects Against Catecholamine-Induced Arrhythmia and Preserves Contractile Function After Myocardial Infarction. *Circ Res.* 2017; 120:120–132. [PubMed: 27799254]
15. Schrickel JW, Brixius K, Herr C, Clemen CS, Sasse P, Reetz K, Grohé C, Meyer R, Tiemann K, Schröder R, Bloch W, Nickenig G, Fleischmann BK, Noegel AA, Schwinger RHG, Lewalter T. Enhanced heterogeneity of myocardial conduction and severe cardiac electrical instability in annexin A7-deficient mice. *Cardiovasc Res.* 2007; 76:257–68. [PubMed: 17662970]
16. Ivanyuk D, Budash G, Zheng Y, Gaspar JA, Chaudhari U, Fatima A, Bahmanpour S, Grin VK, Popandopulo AG, Sachinidis A, Hescheler J, Šari T. Ascorbic Acid-Induced Cardiac Differentiation of Murine Pluripotent Stem Cells: Transcriptional Profiling and Effect of a Small Molecule Synergist of Wnt/ β -Catenin Signaling Pathway. *Cell Physiol Biochem.* 2015; 36:810–30. [PubMed: 26021268]
17. Halbach M, Pillekamp F, Brockmeier K, Hescheler J, Müller-Ehmsen J, Reppel M. Ventricular slices of adult mouse hearts--a new multicellular in vitro model for electrophysiological studies. *Cell Physiol Biochem.* 2006; 18:1–8. [PubMed: 16914885]
18. Neyton J, Miller C. Potassium blocks barium permeation through a calcium-activated potassium channel. *J Gen Physiol.* 1988; 92:549–67. [PubMed: 3235973]
19. Lee CH, Ruben PC. Interaction between voltage-gated sodium channels and the neurotoxin, tetrodotoxin. *Channels (Austin).* 2:407–12.
20. van den Borne SWM, Diez J, Blankesteyn WM, Verjans J, Hofstra L, Narula J. Myocardial remodeling after infarction: the role of myofibroblasts. *Nat Rev Cardiol.* 2010; 7:30–7. [PubMed: 19949426]
21. Priori SG, Blomström-Lundqvist C, Mazzanti A, Blom N, Borggrefe M, Camm J, Elliott PM, Fitzsimons D, Hatala R, Hindricks G, Kirchhof P, Kjeldsen K, Kuck K-H, Hernandez-Madrid A, Nikolaou N, Norekvål TM, Spaulding C, Van Veldhuisen DJ. 2015 ESC Guidelines for the management of patients with ventricular arrhythmias and the prevention of sudden cardiac death. *Eur Heart J.* 2015; 36:2793–2867. [PubMed: 26320108]
22. Eltzschig HK, Eckle T. Ischemia and reperfusion--from mechanism to translation. *Nat Med.* 2011; 17:1391–401. [PubMed: 22064429]
23. Vinten-Johansen J. Involvement of neutrophils in the pathogenesis of lethal myocardial reperfusion injury. *Cardiovasc Res.* 2004; 61:481–97. [PubMed: 14962479]
24. Baxter GF. The neutrophil as a mediator of myocardial ischemia-reperfusion injury: time to move on. *Basic Res Cardiol.* 2002; 97:268–75. [PubMed: 12111036]
25. van Rijen HVM, Eckardt D, Degen J, Theis M, Ott T, Willecke K, Jongasma HJ, Opthof T, de Bakker JMT. Slow conduction and enhanced anisotropy increase the propensity for ventricular tachyarrhythmias in adult mice with induced deletion of connexin43. *Circulation.* 2004; 109:1048–55. [PubMed: 14967725]
26. Vanhoutte D, Schellings M, Pinto Y, Heymans S. Relevance of matrix metalloproteinases and their inhibitors after myocardial infarction: a temporal and spatial window. *Cardiovasc Res.* 2006; 69:604–13. [PubMed: 16360129]
27. Midwinter RG, Vissers MC, Winterbourn CC. Hypochlorous acid stimulation of the mitogen-activated protein kinase pathway enhances cell survival. *Arch Biochem Biophys.* 2001; 394:13–20. [PubMed: 11566022]
28. Carmeliet E. Cardiac ionic currents and acute ischemia: from channels to arrhythmias. *Physiol Rev.* 1999; 79:917–1017. [PubMed: 10390520]
29. Betsuyaku T, Kanno S, Lerner DL, Schuessler RB, Saffitz JE, Yamada KA. Spontaneous and inducible ventricular arrhythmias after myocardial infarction in mice. *Cardiovasc Pathol.* 2004; 13:156–64. [PubMed: 15081472]
30. Gehrman J, Frantz S, Maguire CT, Vargas M, Ducharme A, Wakimoto H, Lee RT, Berul CI. Electrophysiological characterization of murine myocardial ischemia and infarction. *Basic Res Cardiol.* 96:237–50.

31. Cascio WE, Yang H, Muller-Borer BJ, Johnson TA. Ischemia-induced arrhythmia: the role of connexins, gap junctions, and attendant changes in impulse propagation. *J Electrocardiol.* 2005; 38:55–9. [PubMed: 16226075]
32. Danik SB, Rosner G, Lader J, Gutstein DE, Fishman GI, Morley GE. Electrical remodeling contributes to complex tachyarrhythmias in connexin43-deficient mouse hearts. *FASEB J.* 2008; 22:1204–12. [PubMed: 17984180]
33. Greener ID, Sasano T, Wan X, Igarashi T, Strom M, Rosenbaum DS, Donahue JK. Connexin43 gene transfer reduces ventricular tachycardia susceptibility after myocardial infarction. *J Am Coll Cardiol.* 2012; 60:1103–10. [PubMed: 22883636]
34. Lau D, Mollnau H, Eiserich JP, Freeman BA, Daiber A, Gehling UM, Brümmer J, Rudolph V, Münzel T, Heitzer T, Meinertz T, Baldus S. Myeloperoxidase mediates neutrophil activation by association with CD11b/CD18 integrins. *Proc Natl Acad Sci U S A.* 2005; 102:431–6. [PubMed: 15625114]
35. Klinka A, Nussbaum C, Kubala L, Friedrichs K, Rudolph TK, Rudolph V, Paust H-J, Schröder C, Benten D, Lau D, Szocs K, Furtmüller PG, Heeringa P, Sydow K, Duchstein H-J, Ehmke H, Schumacher U, Meinertz T, Sperandio M, Baldus S. Myeloperoxidase attracts neutrophils by physical forces. *Blood.* 2011; 117:1350–8. [PubMed: 20980678]

Nonstandard Abbreviations and Acronyms

MPO	Myeloperoxidase
VT	Ventricular tachycardia
I/R	Ischemia and reperfusion
PI	Permanent ischemia
Cx43	Connexin43
iPSCM	Induced pluripotent stem-cell-derived cardiomyocytes
MAPK	Mitogen-activated protein kinases
LAD	Ligation of the left anterior descending artery
WT	Wild type
MMP	Matrix metalloproteinases
LV	Left ventricular
LVEDD	Left ventricular enddiastolic diameter
EF	Ejection fraction
PMN	Polymorphonuclear leukocytes
CD11b	Integrin alpha M
APD_x	Action potential duration at x% of repolarization
TTX	Tetrodotoxin
PAI-1	Plasminogen activator inhibitor-1

Novelty and Significance

What Is Known?

- Myeloperoxidase (MPO) is released by infiltrating polymorphonuclear neutrophils and has traditionally been viewed as a microbicidal enzyme.
- Accumulating evidence demonstrates involvement of MPO in cardiovascular disease, including atherosclerosis and myocardial disease.
- Even with optimal medical therapy according to current standards life-threatening arrhythmias caused by left ventricular remodeling are a major healthcare concern.

What New Information Does This Article Contribute?

- MPO promotes proarrhythmogenic remodeling in different models of myocardial ischemia and increases vulnerability for ventricular tachycardia in this setting.
- MPO augments post-infarct connexin43 degradation via matrix metalloproteinase 7 activation, aggravates fibroblast-to-myofibroblast transdifferentiation via p38 MAP-kinase phosphorylation and increases post-infarct collagen deposition and fibrosis development.
- MPO deficiency decreases heterogeneity of electrical conduction and reduces conduction block, thereby reducing the development of reentry circuits.

Despite intensive scientific efforts ischemic heart disease is still a leading cause of morbidity and mortality in western countries. Electrical and structural remodeling of the left ventricle following myocardial infarction is the most common substrate for ventricular tachycardia and subsequent sudden cardiac death. In this context, the discovery of new potential therapeutic targets is urgently required. Myeloperoxidase (MPO) was recently identified as predictor of cardiovascular disease. Herein we identify MPO as a promoter for ventricular tachycardia vulnerability via post-infarct connexin43 degradation and fibrosis and subsequent ventricular conduction inhomogeneity. MPO may therefore emerge as a novel therapeutic target for pharmacologic- anti-arrhythmic therapies after myocardial infarction.

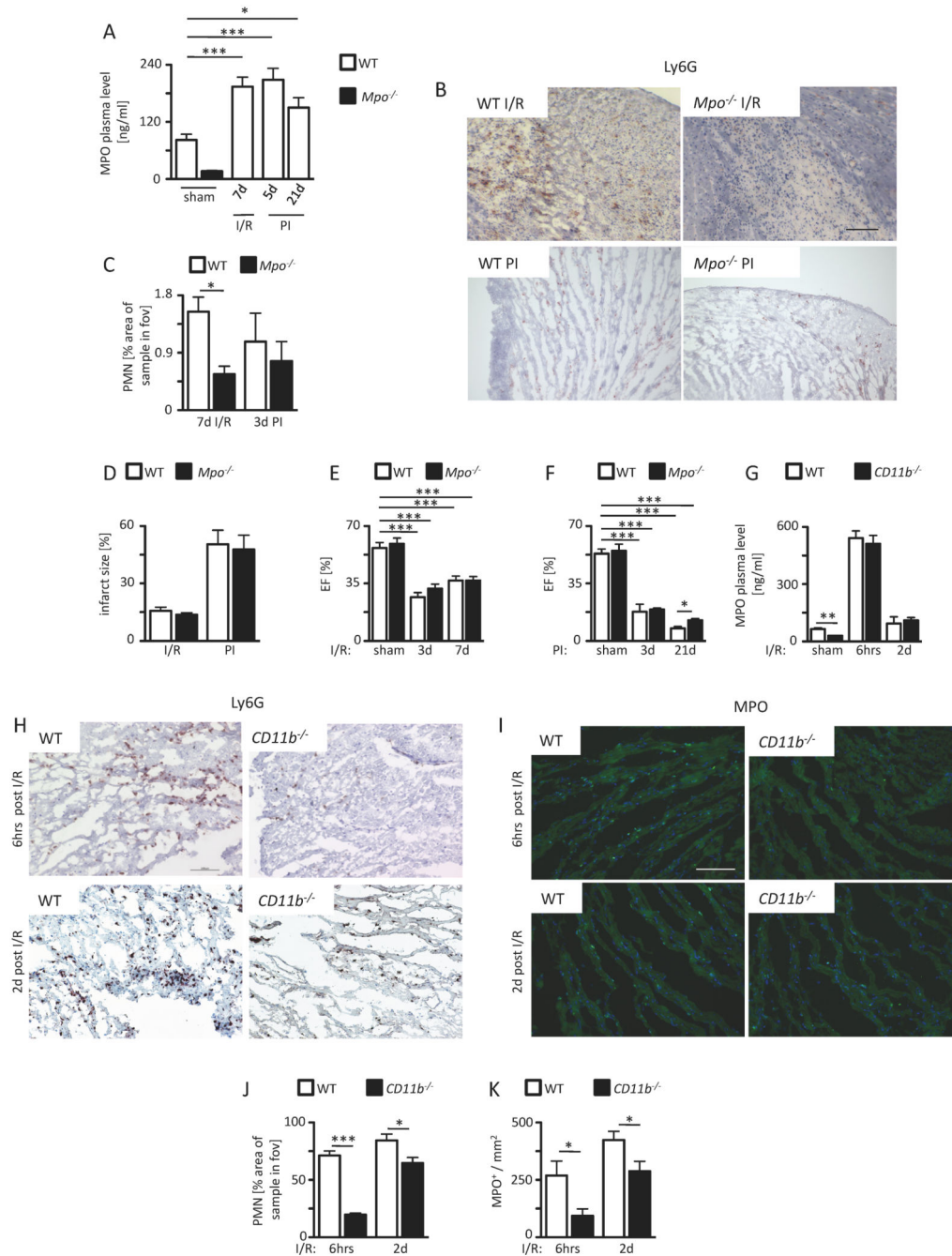


Figure 1.

A) MPO plasma level of sham WT and *Mpo*^{-/-} mice or WT mice after left ventricular ischemia and 7 days of reperfusion (I/R) and 5 and 21 days upon permanent ischemia (PI) as assessed by ELISA. WT sham n=28, *Mpo*^{-/-} sham n=8, WT I/R n=30, WT 5 days PI n=5, WT 21 days n=7. Infiltration of PMN. (B) Immunohistochemical Ly6G stainings (brown) of WT and *Mpo*^{-/-} hearts subjected to I/R or PI. (C) Quantitative analysis of Ly6G+ cells into the infarct and periinfarct zones of WT and *Mpo*^{-/-} hearts after I/R and PI. Scale bar = 200 μm. WT I/R / *Mpo*^{-/-} I/R n=7/13; WT PI / *Mpo*^{-/-} PI n=6/7. Infarct size and left ventricular

function. (D) Infarct size in WT and Mpo^{-/-} hearts after 7 days I/R and 21 days upon PI. WT / Mpo^{-/-} I/R n=6/5; WT / Mpo^{-/-} PI n=6/6. Ejection fraction (EF) after (E) 3 and 7 days I/R or (F) 3 days and 21 days PI of WT and Mpo^{-/-} animals. E: WT / Mpo^{-/-} sham n=4, WT / Mpo^{-/-} 3d I/R n=5/4, WT / Mpo^{-/-} 7d I/R n=8/5; F: WT / Mpo^{-/-} sham n=4, WT / Mpo^{-/-} 3d PI n=5/3, WT / Mpo^{-/-} 21d PI n=4/3.

Infiltration of PMN and accumulation of MPO. (G) MPO plasma levels of WT and CD11b^{-/-} mice subjected to ischemia following 6 hours or 2 days of reperfusion. (H, J) Immunohistochemical Ly6G stainings (brown) and quantitative analysis of Ly6G⁺ cells into the infarct and periinfarct zones of WT and CD11b^{-/-} hearts and (I, K) immunofluorescence MPO stainings (light green) and quantitative analysis of MPO immunoreactivity in WT and CD11b^{-/-} hearts subjected to ischemia following 6 hours or 2 days of reperfusion. G: WT / CD11b^{-/-} sham n=5/5, WT / CD11b^{-/-} 6h I/R n=5/5, WT / CD11b^{-/-} 2d I/R n=3/7; J: WT / CD11b^{-/-} 6h I/R n=3/4, WT / CD11b^{-/-} 2d I/R n=5/5; K: WT / CD11b^{-/-} 6h I/R n=5/5, WT / CD11b^{-/-} 2d I/R n=5/7. *= $P < 0.05$, ***= $P < 0.001$, Kruskal Wallis test followed by Bonferroni post hoc test. Mean \pm SEM is shown.

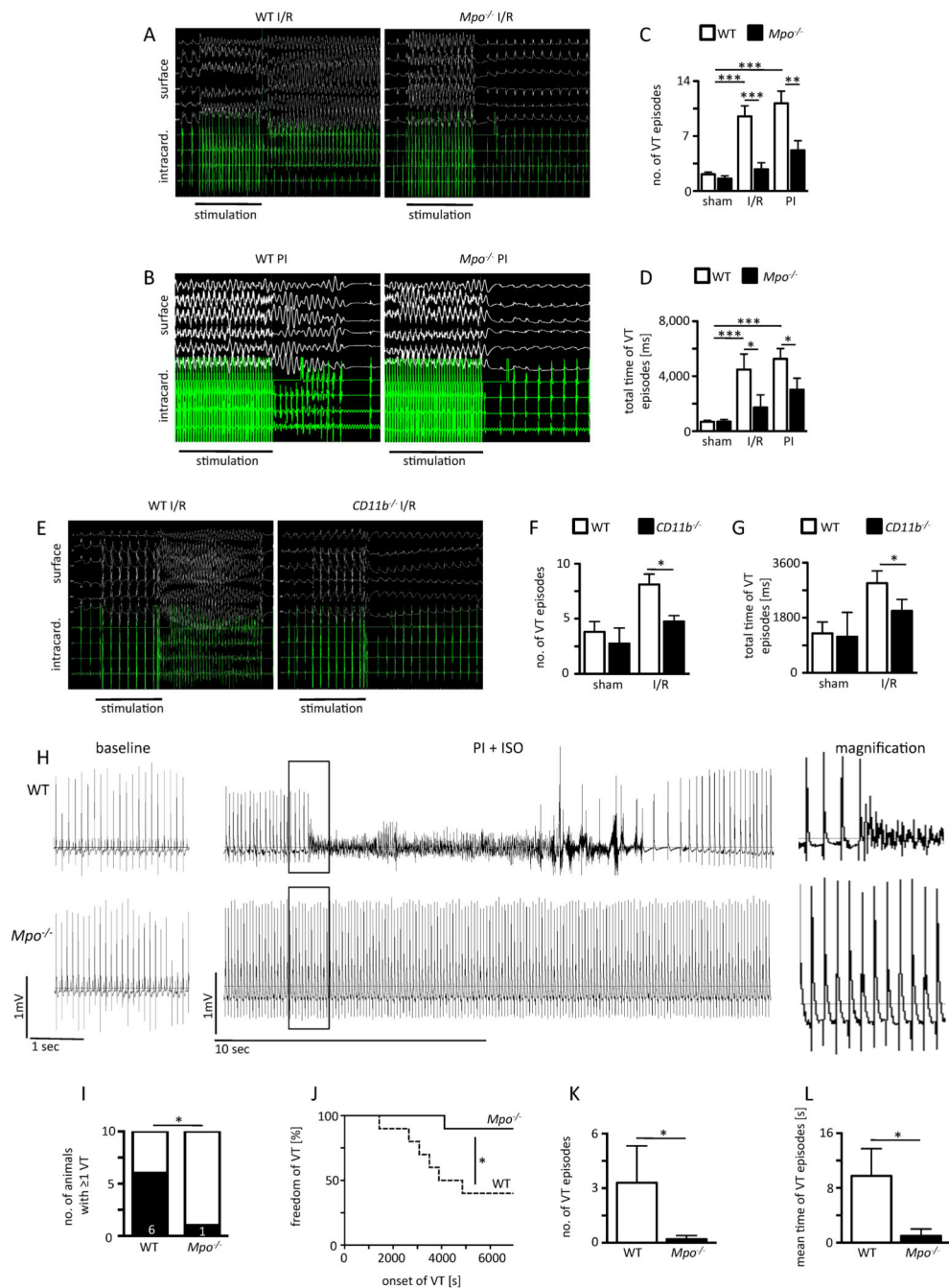


Figure 2. Vulnerability to ventricular arrhythmias: Representative surface (top panel) and intracardiac (bottom panel)

ECG recordings of electrical ventricular stimulation of WT and Mpo^{-/-} mice after (A) ischemia and 7 days of reperfusion (I/R) and (B) 21 days upon permanent ischemia (PI). (C) Number of episodes of ventricular tachycardia (VT) and (D) total time of VT after I/R and PI. (E) Representative ECG recordings of WT and CD11b^{-/-} mice after ischemia following 2 days of reperfusion. (F) Number of VT episodes and (G) total time of VT in WT and CD11b^{-/-} mice after ischemia following 2 days of reperfusion. sham: n=4; C, D: WT / Mpo^{-/-} I/R n=8/9; WT / Mpo^{-/-} PI n=6/11; F, G: sham n=11/4, WT / CD11b^{-/-} I/R n=9/8.

Analysis of ventricular tachycardia 24 hrs after LAD-ligation: (H) Representative ECG-traces recorded by telemetry investigations (for 2 hrs) before (left panel) and 24 hrs after LAD-ligation and two Isoproterenol injections (2 mg/kg BW) (middle panel) in WT and Mpo^{-/-} animals. Magnification of the highlighted section is shown in the right panel. Analyses of (I) VT probability, (J) onset of VT, (K) mean number of VT episodes and (L) mean time of VT episodes in WT and Mpo^{-/-} animals. n=10/10. * $P < 0.05$, ** $P < 0.01$, *** $P < 0.001$, by Kruskal Wallis test followed by Bonferroni post hoc test. (I) Chi-square test. (J) Log-rank test.

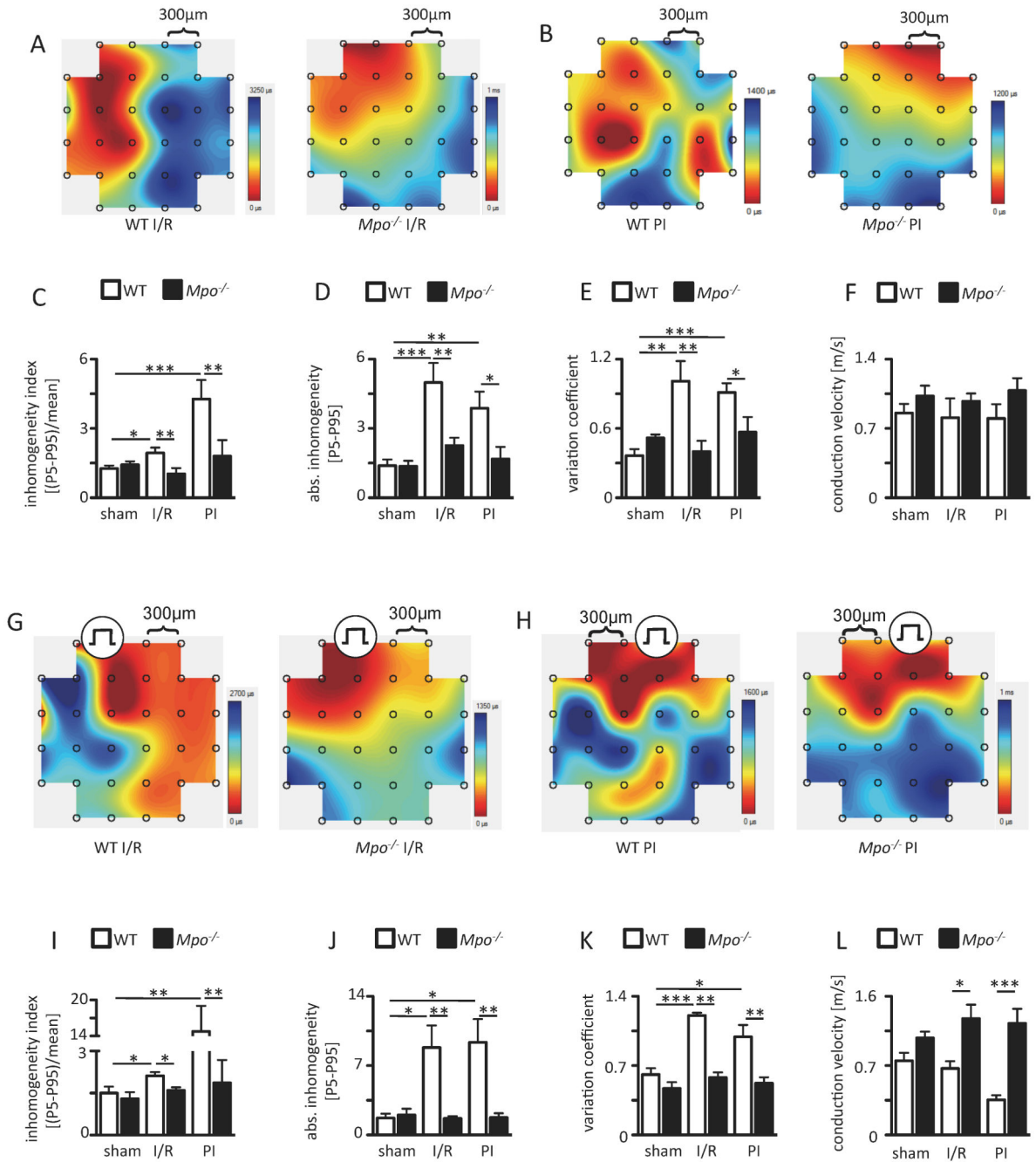


Figure 3. Epicardial mapping analyses. Representative maps of spontaneous conduction in the periinfarct region of WT and *Mpo*^{-/-} hearts

(A) after left ventricular ischemia and 7 days of reperfusion (I/R) and (B) 21 days upon permanent ischemia PI (from dark red to dark blue, bars indicate total time from first to last measurement within one heartbeat). (C) Inhomogeneity index, (D) absolute inhomogeneity, (E) variation coefficient of conduction and (F) mean conduction velocity of WT and *Mpo*^{-/-} hearts. sham n=5; WT I/R / *Mpo*^{-/-} I/R n=6/6; WT PI / *Mpo*^{-/-} PI n=7/5. Representative conduction maps of stimulated WT and *Mpo*^{-/-} hearts subjected to (G) I/R or (H) PI with indicated pacing position. (I) Inhomogeneity index, (J) absolute inhomogeneity, (K)

variation coefficient and of conduction and (L) mean conduction velocity in WT and Mpo^{-/-} hearts subjected to I/R or PI. Mean \pm SEM is shown; sham WT / Mpo^{-/-} n=3/4; WT / Mpo^{-/-} I/R n=5/6; WT / Mpo^{-/-} PI n=5/7. *=P<0.05, **=P<0.01, ***=P<0.001, by Kruskal Wallis test followed by Bonferroni post hoc test.

Author Manuscript

Author Manuscript

Author Manuscript

Author Manuscript

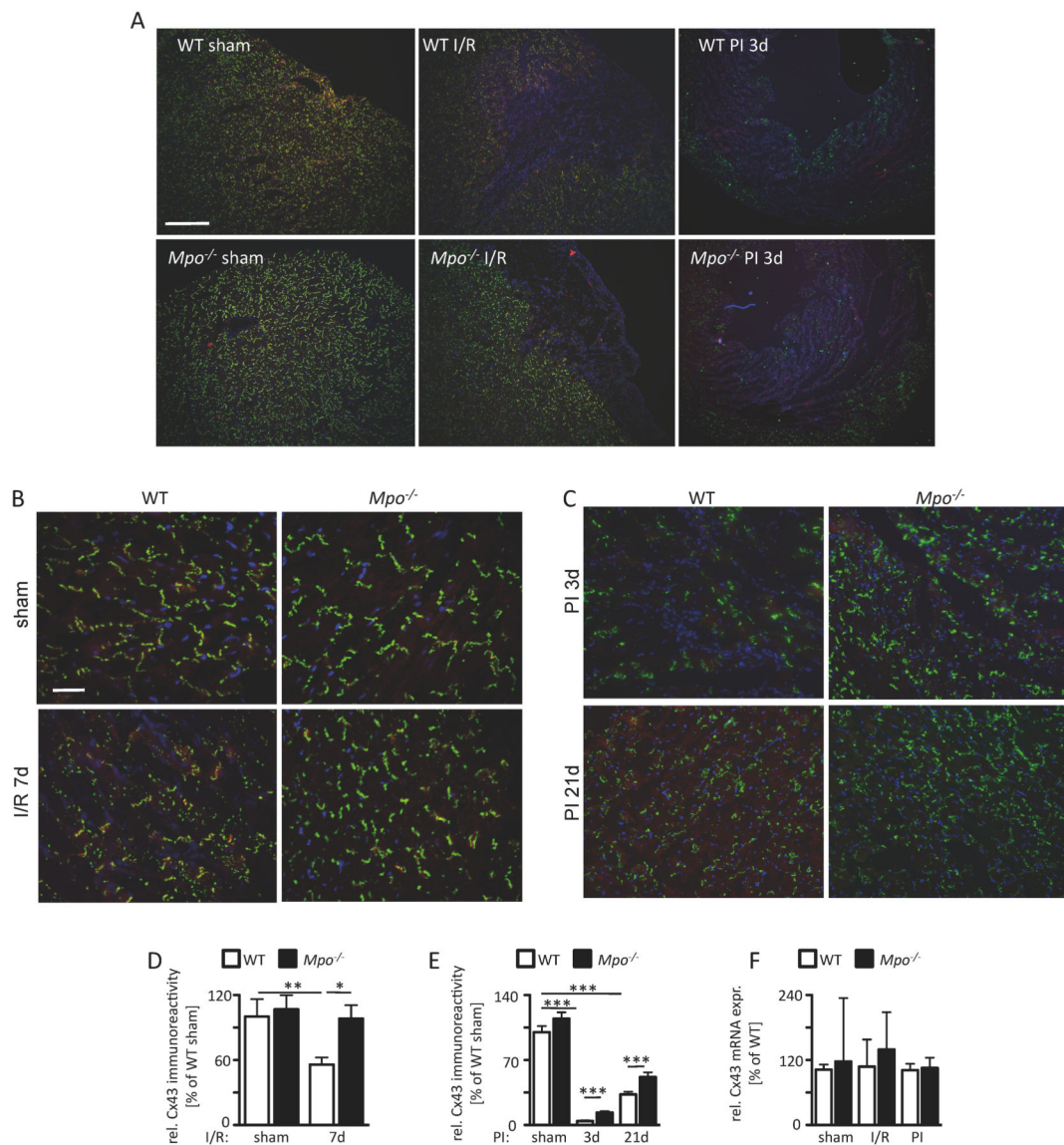


Figure 4. Connexin43 (Cx43) integrity. (A) Immunoreactivity for Cx43 in cardiac sections of WT and Mpo^{-/-} mice after left ventricular ischemia and 7 days of reperfusion (I/R) and 3 and 21 days upon PI (green=Cx43, red=N-cadherin, blue=DAPI; scale bar=200 μ m)

Immunoreactivity for Cx43 and N-cadherin in the cardiac periinfarct zone of WT and Mpo^{-/-} animals subjected to (B) sham-operation and 7 days I/R or (C) 3 and 21 days PI (red=N-cadherin, green=Cx43, blue=DAPI; scale bar=30 μ m). (D) Quantitative analysis of Cx43 immunoreactivity in the periinfarct zone of WT- and Mpo^{-/-} mice upon I/R or (E) 3 and 21 days PI (C: WT / Mpo^{-/-} sham n=9/4, WT / Mpo^{-/-} 7d I/R n=7/11; D: WT / Mpo^{-/-} sham n=6/11, WT / Mpo^{-/-} 3d PI n=6/7, WT / Mpo^{-/-} 21d PI n=6/7. (F) Analysis of left ventricular Cx43 mRNA expression of sham, I/R or PI hearts of WT and Mpo^{-/-} mice. n=3 for all groups. *= $P < 0.05$, **= $P < 0.01$, ***= $P < 0.001$, by Kruskal Wallis test followed by Bonferroni post hoc test. Mean \pm SEM is shown.

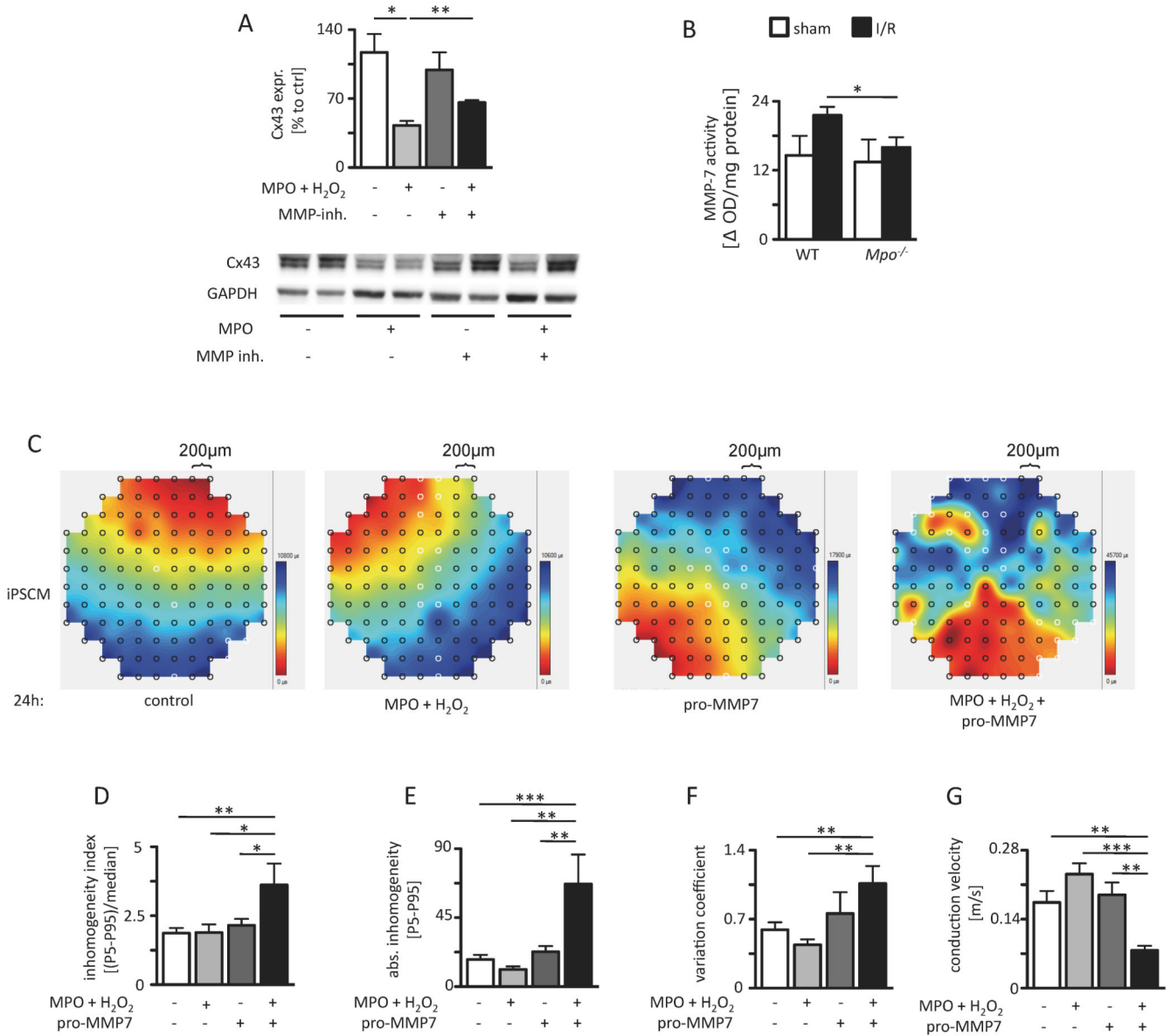


Figure 5. MPO-dependent effect of MMP-7 on Cx43 and electrical homogeneity. (A) Immunoblot analyses of Cx43 in isolated cardiomyocytes upon MPO treatment with and without additional MMP-inhibitor treatment (sham: n=4; MPO: n=4; MMP-inhibitor: n=4; MPO/MMP-inhibitor: n=3, the original immunoblot is shown in Online Figure VIII)

(B) MMP-7 activity in the periinfarct region of I/R WT and *Mpo*^{-/-} hearts (WT / *Mpo*^{-/-} sham n=5/5, WT / *Mpo*^{-/-} I/R n=10/8). (C) Representative maps of spontaneous conduction of iPSCM treated with NaCl (control), MPO/H₂O₂, pro-MMP-7 or MPO/H₂O₂/pro-MMP-7 with analysis of (D) inhomogeneity index, (E) enhanced absolute inhomogeneity, (F) variation coefficient of conduction and (G) conduction velocity. Control: n=11, MPO/H₂O₂: n=5, pro-MMP-7: n=5, MPO/H₂O₂/pro-MMP-7: n=7. *=*P*<0.05, **=*P*<0.01, by Kruskal Wallis test followed by Bonferroni post hoc test. Mean ± SEM is shown.

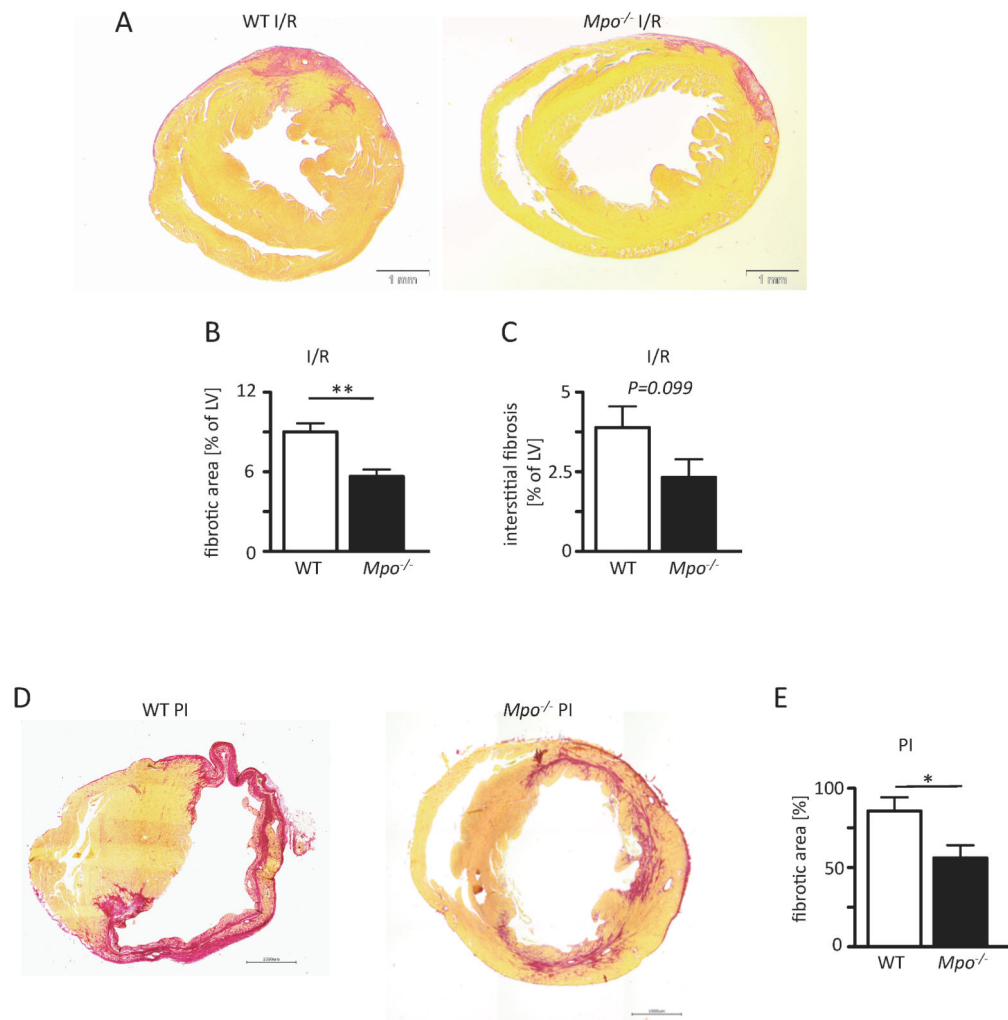


Figure 6. MPO-dependent fibrotic remodeling. Picrosirius red stained cardiac sections of WT and *Mpo*^{-/-} mice

(A) upon ischemia and 7 days of reperfusion (I/R) or (D) 21 days of permanent ischemia (PI) with red areas indicating collagen deposition and analysis of (B) total left ventricular fibrotic area and (C) interstitial fibrosis; B,C: WT / *Mpo*^{-/-} 7d I/R n=6/7 and (E) total left ventricular fibrosis after PI of WT and *Mpo*^{-/-} hearts. Mean ± SEM is shown; WT / *Mpo*^{-/-} 21d PI n=7/9. Scale bar = 1mm. *=*P*<0.05, **=*P*<0.01, by unpaired Student's t-test.

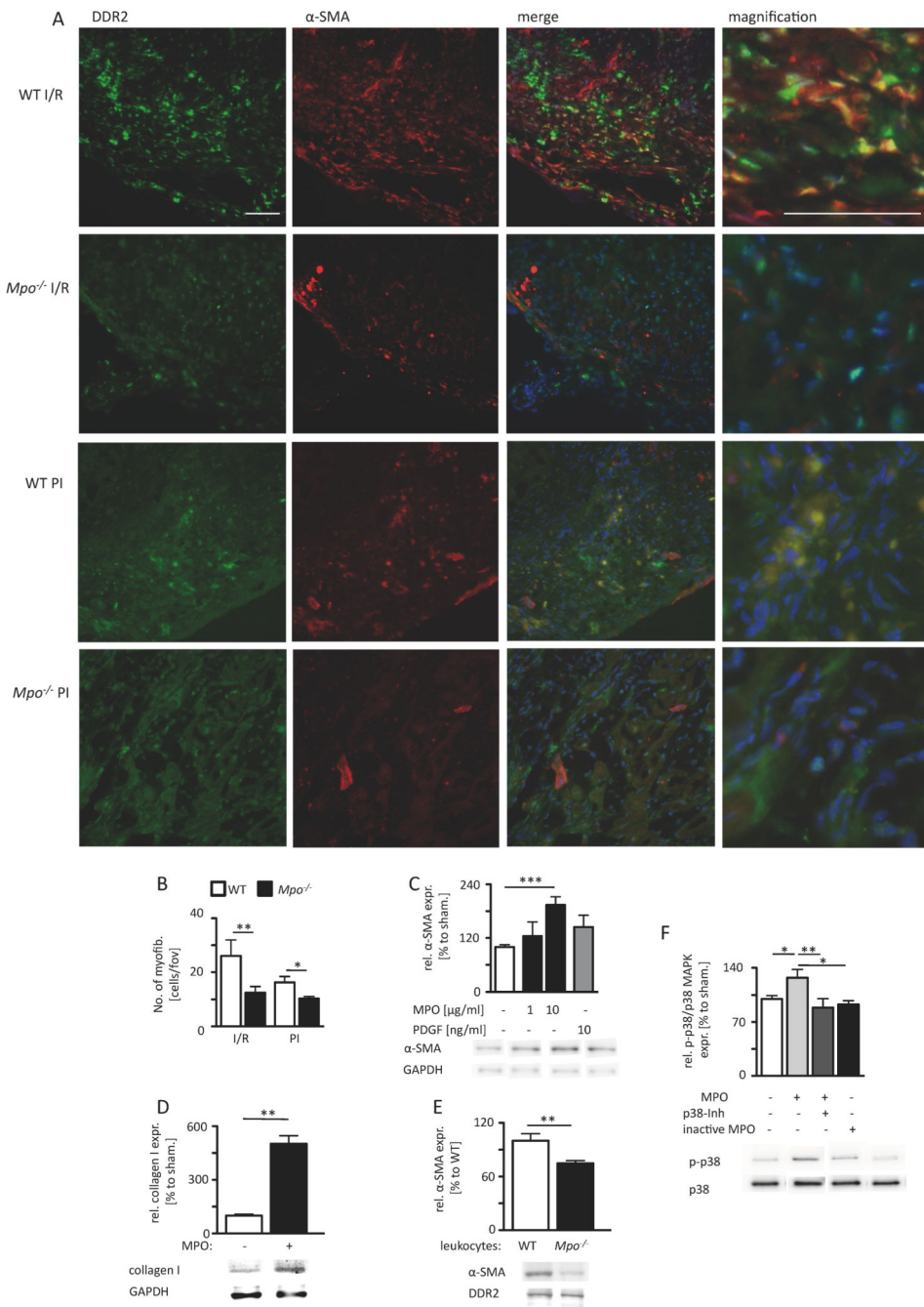


Figure 7. MPO-dependent fibroblast transdifferentiation

(A) Representative immunofluorescence stainings for fibroblast marker DDR2 (green) and myofibroblast marker α -SMA (red) within the infarct area of WT and *Mpo*^{-/-} mice after left ventricular ischemia and 7 days of reperfusion (I/R) and 5 days of permanent ischemia (PI) (blue=DAPI; scale bar=200 μ m). (B) Quantitative analysis of myofibroblasts within the infarct and periinfarct region after 7 days of I/R and 5 days PI; WT / *Mpo*^{-/-} 7d I/R n=11/15, WT / *Mpo*^{-/-} 5d PI n=5/5. (C) Relative α -SMA protein expression of isolated cardiac fibroblasts after 8 hours of MPO and PDGF treatment. (D) Relative collagen I expression of

isolated cardiac fibroblasts after 36 hours of MPO treatment. (E) Relative α -SMA protein expression of isolated cardiac fibroblasts after co-culture with WT or Mpo^{-/-} leukocytes. (F) Relative phosphorylation of p38 MAP-kinase (p-p38/p38 MAPK) in isolated fibroblasts upon 15 minutes of MPO treatment. Original immunoblots are shown in Online Figure IX-XII. Mean \pm SEM is shown. C, D, E, F: n=4 independent experiments. *= $P < 0.05$, **= $P < 0.01$, ***= $P < 0.001$, by unpaired Student's t-test for B, D, E and by Kruskal Wallis test followed by Bonferroni post hoc test for C, F.

Table 1

Baseline characteristics of patients.

Variable	All (n=2622)	Arrhythmias negative (n=2448)	Arrhythmias positive (n=174)	p
Age (years)	62.1±10.6	62±10.6	63.7±11.3	0.03
Male sex (%)	65	65	69	0.311
Diabetes mellitus (%)	30	31	27	0.364
Coronary artery disease (%)	74	74	76	0.569
Former/current smoker (%)	64	63	70	0.107
LV Ejection Fraction (%)	60(50-65)	60(50-65)	55(50-60)	0.014
LDL cholesterol (mg/dL)	98(80-119)	98(80-120)	96(78-116)	0.246
HDL cholesterol (mg/dL)	34(28-41)	34(28-41)	35(28-41)	0.845
ACE inhibitors (%)	44	43	58	<0.001
Beta blocker (%)	60	60	59	0.988
Statin (%)	57	57	61	0.314
Aspirin (%)	75	75	74	0.861
MPO (pmol/L)	502.5(287.2-914)	496.7(284.5-899.6)	593.1(359.8-1014.4)	0.004

Table 2

Unadjusted and adjusted Odds Ratio for history of ventricular arrhythmia, sudden cardiac death and/or implantable cardioverter defibrillator. Adjusted for age, sex, systolic blood pressure, low-density lipoprotein, high-density lipoprotein, smoking, diabetes, coronary artery disease, and left ventricular ejection fraction.

Serum MPO	Tertile 1	Tertile 2	Tertile 3
Range	<354.1	354.1-736.23	>=736.23
Unadjusted OR	1	1.33 (0.88-1.99)	1.76 (1.19-2.6) **
Adjusted OR	1	1.38 (0.92-2.09)	1.83 (1.23-2.73) **
Event rate	43/864=4.98	58/893=6.49	73/865=8.44

** $P < 0.01$, by binary logistic regression analysis.